Communs geol. Surv. Namibia, **10** *(1995), 21-32*

Geochemistry of granitic in-situ low-melt fractions - an example from the Central Damara Orogen

S. Jung[1], E. Hoffer[1], P. Masberg[1] and S. Hoernes[2]

[1]*Institut für Mineralogie, Kristallographie und Petrologie, Lahnberge, 35032 Marburg/Lahn, Germany*

[2]*Mineralogisch-Petrologisches lnstitut der Universität Bonn, Poppelsdorfer Schloß, 53115 Bonn, Germany*

Migmatites outcropping along the Omaruru River in the central Damara Orogen of Namibia are the product of both the injection of granitic material and *in-situ* partial melting of mainly pelitic greywackes. This partial melting event is mainly due to heat transfer from intruding granites during orogenic decompression at high temperatures. Anatexis under vapour-absent conditions in the deeper crust leads to dehydration melting of biotite in pelites and, to a lesser extent, in metagreywackes generating peraluminous garnet- and cordierite-bearing S-type granites which subsequently evolved through a complex assimilation and fractional crystallisation history (AFC). Anatexis under vapour-present conditions leads to the formation of in-situ leucosomes which are formed by disequilibrium melting of pelitic greywackes at T=690-710°C, P=4.6-5.5 kbar, X_{H2O}=0.9 and f_{02} between the QFM and NNO buffers. Disequilibrium melting is the favoured process for generation of the in-situ leucosomes and is probably related to an overstep of the wet solidus during infiltration of an aqueous fluid liberated from the crystallizing granites. The occurrence of contemporaneous hornblende-bearing granites with A-type affinities is probably linked with exhumation and uplift late in the tectono-metamorphic history.

Introduction

Recently there has been considerable revival of interest in the origin of granitic rocks, and in particular, the relationship between granite genesis and migmatization. Among the various mechanisms proposed to account for the diverse types of migmatites, partial melting and melt segregation remain the main genetic processes of migmatization. Dehydration melting of hydrous phases in pelites and metagreywackes (Thompson, 1982; Clemens and Vielzeuf, 1987; LeBreton and Thompson, 1988; Vielzeuf and Holloway, 1988; Holtz and Barbey, 1991; Holtz and Johannes, 1991) coupled with sequential melting and restite unmixing is an attractive model for the generation of peraluminous granitic magmas as it is an intracrustal process that can account for the differentiated nature of crustal segments and for the water-undersaturated nature of most granitic magmas. Nevertheless, the question of whether the trace element signature of melts and residues is consistent with that model remains open to debate. Among the numerous geochemical studies of granitic magmas, the idea that different geochemical characteristics of granites are related to different source rock compositions has often been emphasized, and has also been demonstrated experimentally (Conrad *et al.*, 1988; Holtz and Johannes, 1991). However, important geochemical differences can also be related to the presence of different amounts of residual minerals in the magmas. This is especially true for Fe, Mg and Ti (and related trace elements) and therefore, crustal peraluminous granites containing high amounts of these elements should be rich in residual mafic phases. On the other hand, leucogranites correspond either to pure melts extracted from their source or to residual magmas in which separation of early crystallized phases has occurred (e.g. Price, 1983). Among the leucogranites generated by partial melting of crustal rocks, there are strong geochemical differences especially with respect to K, Na (and related trace elements), and to a lesser extent, with respect to Al and Si. The geochemical variability of these leucogranites is considered to reflect different source rock compositions, different stages of magmatic differentiation or different anatectic conditions (P, T, X_{H2O}, f_{02}) in the same source rock. In a recent review paper, Brown (1993) pointed out the need for detailed investigations on mineral reactions in natural pelitic migmatites as an essential step towards understanding not only the metamorphic petrogenesis of these rocks but also the origin of peraluminous granites in continental settings. The aluminous migmatites and the peraluminous granitic rocks (intrusive and *in-situ*) from the Omaruru River in the central Damara Orogen of Namibia show several features relevant to these problems. This paper discusses several phenomena of *in-situ* migmatization in connection with intrusion of peraluminous granites which were generated in the lower crust and intruded in high-grade metasediments to form vein-like migmatites.

Geological setting and field relations

The migmatitic complex studied is located in the Omaruru River at 14.95° E and 21.50° S in the central Damara Orogen, Namibia and consists mainly of migmatites generated by intrusion of granites. The studied granites are syntectonic, medium- to fine-grained leucogranites. Subjected to syn- to post-tectonic upper amphibolite facies metamorphism, the study area is structurally complex and has abundant anatectic features typical of many migmatite terrains. The three main metasedimentary units are psammitic greywackes, pelites and metagreywackes of the Kuiseb Formation. In addition, rare amphibolites, marbles and calc-silicates occur. Intercalated are two types of migmatites, garnet -bearing stromatic migmatites and garnet-free nebulitic migmatites. Psammitic greywackes do not show any mineralogical and geochemical evidence of partial melting and are not considered further. Me-

Table 1.: Composition (in wt. %) of selected minerals from migmatites, garnet-cordierite granites, hornblende granites and one metapelite (Leuco: Leucosome of migmatite, Mel: Melanosome of migmatite, G/C: Garnet-cordierite granite, Hbl: Hornblende granite, MP: Metapelite)

Sample	30/12	30/12	30/12	30/12	12/2	12/2	89/80	89/80	89/19	89/19	89/53-54	89/53-54	89/76	89/76	26/5	26/5	30/12	30/12	12/2
Host rock	Leuco.	Leuco.	Mel.	Mel.	G/C	G/C	G/C	G/C	G/C	G/C	G/C	G/C	G/C	G/C	G/C	G/C	Leuco.	Mel.	G/C
Mineral	Gt 11	Gt 4	Gt 7	Gt 1	Gt 19	Gt 18	Gt 36	Gt 31	Gt 59	Gt 63	Gt 18	Gt 22	Gt 28	Gt 32	Gt 52	Gt 54	Bio 14	Bio 15	Bio 71
	core	rim	core	rim	core	rim	core	rim	core	rim	core	rim	core	rim	core	rim			
SiO2	36,60	36,39	36,27	36,47	36,47	35,89	36,76	37,25	35,75	36,02	36,61	37,08	36,41	36,82	36,81	35,76	35,25	35,26	34,77
TiO2	0,00	0,00	0,00	0,00	0,00	0,00	0,00	0,00	0,00	0,00	0,00	0,00	0,00	0,00	0,00	0,00	1,63	3,99	3,60
Al2O3	20,90	20,95	20,86	20,76	20,77	20,36	20,66	20,73	20,68	20,46	20,94	20,86	20,80	20,50	20,25	20,82	20,75	19,55	18,76
Fe2O3	0,00	0,00	0,00	0,00	0,00	0,00	0,00	0,00	0,00	0,00	0,00	0,00	0,00	0,00	0,00	0,00	1,23	0,00	0,00
FeO	31,10	31,10	34,10	33,86	32,95	32,74	37,15	37,25	35,87	36,22	33,70	32,78	34,66	34,61	34,08	34,40	19,53	18,92	20,53
MnO	5,89	5,88	3,64	3,76	8,23	8,78	1,63	1,98	3,26	3,60	6,14	6,46	5,08	5,22	5,58	6,20	0,05	0,16	0,19
MgO	3,85	3,89	3,10	2,97	2,85	1,50	2,97	2,87	2,62	2,20	2,57	2,16	2,35	2,15	2,50	1,80	9,08	7,49	7,82
CaO	0,79	0,79	0,87	0,77	0,31	0,30	0,91	0,84	0,68	0,60	0,61	0,66	0,53	0,50	0,57	0,68	0,00	0,00	0,00
Na2O																	0,16	0,11	0,10
K2O																	9,82	9,81	10,83
H2O																	3,95	3,95	3,95
total	99,13	99,00	98,84	98,59	101,58	99,57	100,08	100,92	98,86	99,10	100,57	100,00	99,83	99,80	99,79	99,66	101,45	99,24	100,55
Al	69,18	69,08	76,50	77,05	70,47	73,29	82,10	81,98	80,17	81,62	74,42	74,45	77,57	78,00	75,85	76,45			
Py	15,28	15,54	12,44	12,04	10,87	5,98	11,70	11,25	10,49	7,80	10,13	8,75	9,38	8,64	9,93	7,14			
Sp	13,29	13,25	8,30	8,67	17,82	19,87	3,65	4,41	7,39	8,84	13,73	14,88	11,53	11,91	12,59	14,47			
Gr	2,26	2,25	2,51	2,24	0,84	0,86	2,49	2,26	1,95	1,74	1,73	1,92	1,52	1,45	1,63	1,94			

Sample	89/80	89/19	89/53-54	89/76	26/5	30/12	12/2	89/80	89/19	89/53-54	89/76	26/5	89/26	30/12	30/12	30/1	89/57	89/15	89/14
Host rock	G/C	G/C	G/C	G/C	G/C	Leuco.	G/C	G/C	G/C	G/C	G/C	G/C	Hbl	Mel.	Leuco.	MP	G/C	Hbl	Hbl
Mineral	Bio 39	Bio 76	Bio 69	Bio 41	Bio 73	Plg 15	Plg 30	Plg 133	Plg 8	Plg 4	Plg 42	Plg 2	Plg 35	Cd 8	Cd 10	Cd 20	Cd 3	Hbl 24	Hbl 1
SiO2	34,65	34,75	34,13	35,03	34,00	61,69	65,24	62,08	64,21	63,50	64,11	63,84	60,57	48,73	47,03	46,94	47,83	40,78	40,15
TiO2	2,83	3,20	3,22	2,69	3,33	0,00	0,00	0,01	0,00	0,00	0,00	0,00	0,00	0,01	0,00	0,00	0,00	1,58	1,62
Al2O3	19,23	19,14	19,29	20,08	19,74	24,82	21,78	23,47	22,50	23,20	23,26	22,77	25,28	32,65	32,33	32,72	29,56	10,44	10,19
Fe2O3	0,00	0,00	0,00	0,00	0,00	0,00	0,00	0,00	0,00	0,00	0,00	0,00	0,00	0,00	0,00	0,00	0,00	0,00	0,00
FeO	22,67	22,13	22,32	21,28	21,95	0,00	0,00	0,04	0,00	0,00	0,00	0,00	0,03	10,18	10,85	8,47	10,35	25,38	24,29
MnO	0,06	0,13	0,26	0,23	0,12	0,00	0,00	0,02	0,00	0,00	0,00	0,00	0,00	0,33	0,49	0,26	0,45	0,98	0,98
MgO	6,85	5,83	6,00	6,96	6,35	0,00	0,00	0,00	0,00	0,00	0,00	0,00	0,01	7,34	6,77	7,59	6,88	4,55	5,02
CaO	0,00	0,00	0,00	0,00	0,00	4,92	2,04	4,43	2,42	3,83	2,94	3,29	6,76	0,00	0,00	0,00	0,00	10,93	10,44
Na2O	0,11	0,11	0,08	0,09	0,15	8,30	10,06	9,23	10,48	9,67	10,27	9,73	7,77	0,34	0,29	0,15	1,21	1,69	1,69
K2O	10,06	10,38	10,53	10,04	10,36	0,34	0,20	0,42	0,13	0,24	0,31	0,25	0,20	0,00	0,00	0,00	0,00	1,73	1,76
H2O	3,95	3,95	3,95	3,95	3,95													1,90	1,90
total	100,41	99,62	99,78	100,35	99,95	100,07	99,32	99,70	99,74	100,44	100,89	99,88	100,62	99,58	97,76	96,13	96,28	99,96	98,04
Ab						73,76	88,85	77,18	88,08	80,97	84,89	83,07	66,78						
Or						2,04	1,18	2,33	0,74	1,31	1,69	1,42	1,12						
An						24,20	9,97	20,48	11,33	17,71	13,43	15,51	32,10						

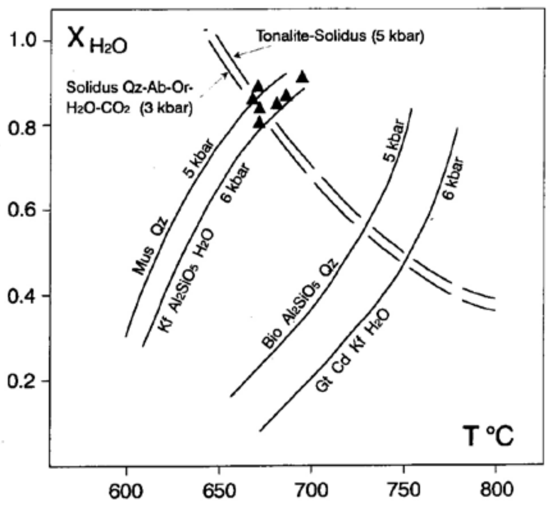

Figure 1: T-X_{H2O} conditions of *in-situ* migmatite formation in the study area as well as conditions of granite formation in the deeper crust. Diagram and location of mineral reaction curves are from Osanai *et al.*(1992). The positions of the triangles reflect PT conditions of granite formation due to the incongruent melting of biotite whereas the circles represent conditions of migmatite formation due to the breakdown of muscovite.

tapelites and metagreywackes are characterised by a continuous banding on a millimetre to centimetre scale defined by alternating, foliated biotite-rich layers and granular quartz-feldspar layers of sedimentary origin. Throughout the complex migmatitic structures are well developed, sometimes with extensive disruption of the banded mesosomes by a fine-grained leucosome bordered locally by a thin biotite-rich melanosome. Dark blue-grey knots of cordierite and large porphyroblasts of garnet are common in those melanosomes and the associated leucosomes. Where migmatization is extensive, the former metasediments take on a nebulitic to schlieren-like character with irregular melanosomes preserved within a cordierite- and biotite-rich matrix in which the distinction between mesosome and leucosome is very difficult.

The granitic melts intrude the migmatised metasediments in the form of planar, sometimes irregular dykes and sheets. The centre of the complex is made up of a leucocratic, nearly restite-free granite. The granitic melts can be roughly divided in four types, namely in two types of leucocratic, coarse- to medium-grained garnet-cordierite granites with different geochemical signatures, in a less abundant light-grey, fine- to medium-grained hornblende-bearing granite and *in-situ* leucosomes.

Petrography

The most common metamorphic mineral assemblage in the complex is biotite-plagioclase-K-feldspar-sillimanite-cordierite-quartz within the pelites and metagreywackes. Pelites have higher modal abundances of biotite, cordierite and sillimanite and lower modal abundances of plagioclase and quartz than metagreywackes. In both rock types, biotite defines the foliation. It is commonly associated with tabular plagioclase, quartz and oxides. Plagioclase occurs as idioblastic to subidioblastic grains more or less evenly distributed throughout the rock. Xenoblastic perthitic microcline shows inclusions of biotite and quartz. Quartz ranges from small rounded inclusions in feldspars and cordierites to coarse-grained patches showing undulose extinction. Cordierite is clear, coarse-grained, tabular, sometimes twinned and contains inclusions of quartz, biotite and sillimanite. Fibrolitic sillimanite is enclosed in cordierite and garnet. Prismatic sillimanite occurs only in some of the granite veins. The metasediments contain only minor amounts of muscovite which may be in part retrograde in origin. More complex metamorphic assemblages are developed in the stromatic garnet-bearing migmatites where garnet grows at the expense of sillimanite, biotite and probably cordierite. Furthermore, muscovite is absent and the development of well defined garnet- and cordierite-bearing leucosomes can be recognized. Garnets are usually larger than the other minerals. Within these garnet-bearing migmatites, cordierite occurs in leucosomes and in melanosomes. In melanosomes, cordierite is texturally identical to that in the metasediments whereas in leucosomes cordierite is often inclusion-free and subhedral. Biotite is concentrated in melanosomes together with cordierite, sillimanite, apatite, zircon and tourmaline. The leucosomes contain plagioclase, quartz and garnet and minor amounts of cordierite, K-feldspar and accessories.

Most of the intrusive granite veins in the area studied are leucocratic, medium- to coarse-grained and contain variable proportions of biotite, garnet and sometimes cordierite. Biotite is the most common mafic phase in the garnet-cordierite granite. Cordierites occur as poikiloblastic inclusion-rich or euhedral nearly inclusion-free crystals. Sillimanite occurs sometimes as interstitial fibrolitic mats or prismatic grains. Garnet is common and occurs either as equigranular to rounded, regularly distributed euhedral crystals which are free from inclusions or as large and irregularly distributed poikilitic crystals with quartz-plagioclase haloes. The former are almost certainly of primary magmatic origin, whereas the latter may be entrained restitic material, either from the lower crust or from the level of emplacement. Within these granite veins plagioclase is generally subhedral and unzoned. These granite-type also contains sporadic perthitic K-feldspar phenocrysts. In the hornblende-bearing granite hornblende dominates over biotite. Proportions of K-feldspar, plagioclase and quartz are variable but the hornblende-bearing granite has a higher modal plagioclase to K-feldspar ratio than the garnet-cordierite granite.

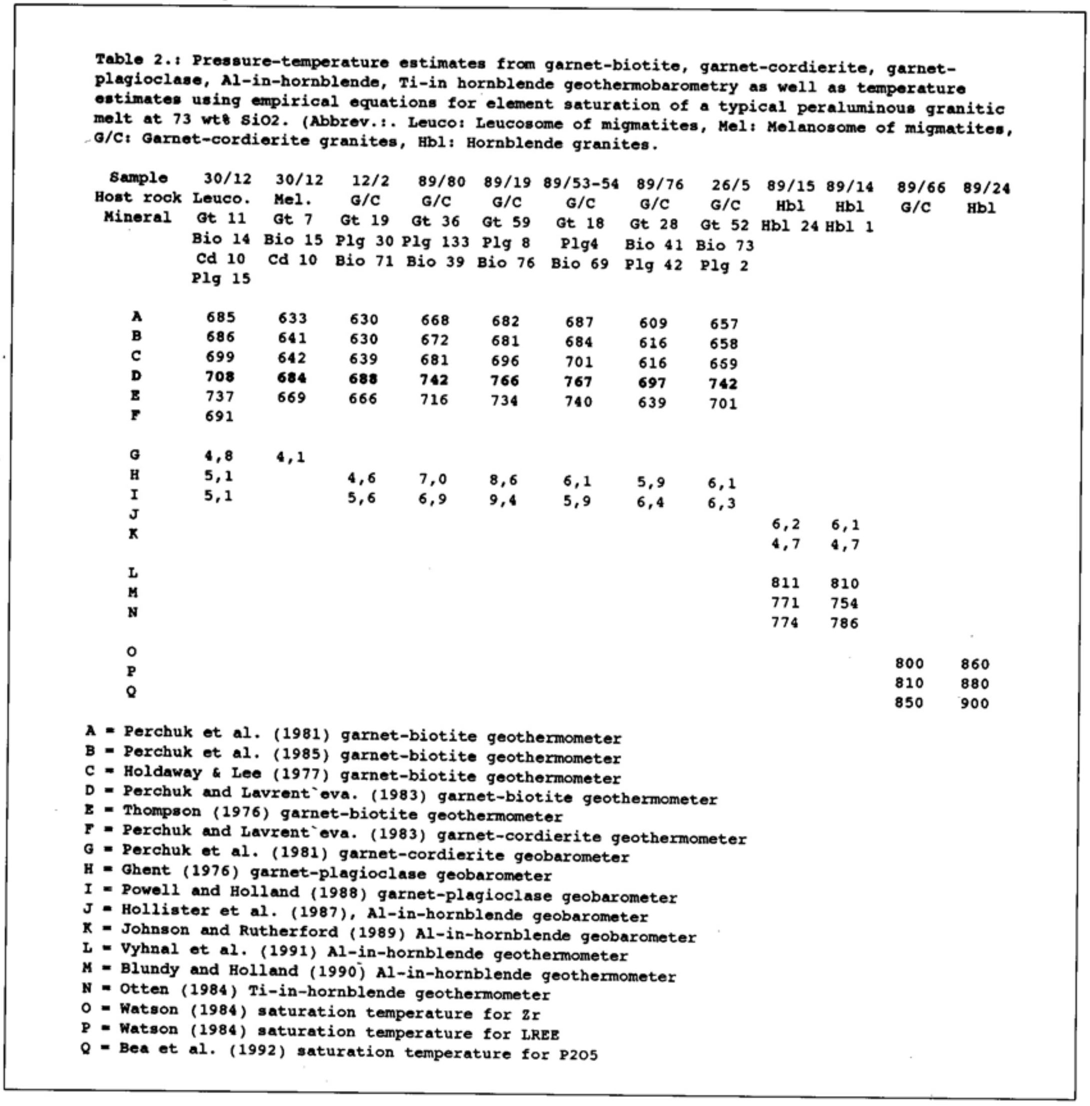

Table 2.: Pressure-temperature estimates from garnet-biotite, garnet-cordierite, garnet-plagioclase, Al-in-hornblende, Ti-in hornblende geothermobarometry as well as temperature estimates using empirical equations for element saturation of a typical peraluminous granitic melt at 73 wt% SiO2. (Abbrev.:. Leuco: Leucosome of migmatites, Mel: Melanosome of migmatites, G/C: Garnet-cordierite granites, Hbl: Hornblende granites.

Sample	30/12	30/12	12/2	89/80	89/19	89/53-54	89/76	26/5	89/15	89/14	89/66	89/24
Host rock	Leuco.	Mel.	G/C	G/C	G/C	G/C	G/C	G/C	Hbl	Hbl	G/C	Hbl
Mineral	Gt 11 Bio 14 Cd 10 Plg 15	Gt 7 Bio 15 Cd 10	Gt 19 Plg 30 Bio 71	Gt 36 Plg 133 Bio 39	Gt 59 Plg 8 Bio 76	Gt 18 Plg4 Bio 69	Gt 28 Bio 41 Plg 42	Gt 52 Bio 73 Plg 2	Hbl 24	Hbl 1		
A	685	633	630	668	682	687	609	657				
B	686	641	630	672	681	684	616	658				
C	699	642	639	681	696	701	616	659				
D	**708**	**684**	**688**	**742**	**766**	**767**	**697**	**742**				
E	737	669	666	716	734	740	639	701				
F	691											
G	4,8	4,1										
H	5,1		4,6	7,0	8,6	6,1	5,9	6,1				
I	5,1		5,6	6,9	9,4	5,9	6,4	6,3				
J									6,2	6,1		
K									4,7	4,7		
L									811	810		
M									771	754		
N									774	786		
O											800	860
P											810	880
Q											850	900

A = Perchuk et al. (1981) garnet-biotite geothermometer
B = Perchuk et al. (1985) garnet-biotite geothermometer
C = Holdaway & Lee (1977) garnet-biotite geothermometer
D = Perchuk and Lavrent`eva. (1983) garnet-biotite geothermometer
E = Thompson (1976) garnet-biotite geothermometer
F = Perchuk and Lavrent`eva. (1983) garnet-cordierite geothermometer
G = Perchuk et al. (1981) garnet-cordierite geobarometer
H = Ghent (1976) garnet-plagioclase geobarometer
I = Powell and Holland (1988) garnet-plagioclase geobarometer
J = Hollister et al. (1987), Al-in-hornblende geobarometer
K = Johnson and Rutherford (1989) Al-in-hornblende geobarometer
L = Vyhnal et al. (1991) Al-in-hornblende geothermometer
M = Blundy and Holland (1990) Al-in-hornblende geothermometer
N = Otten (1984) Ti-in-hornblende geothermometer
O = Watson (1984) saturation temperature for Zr
P = Watson (1984) saturation temperature for LREE
Q = Bea et al. (1992) saturation temperature for P2O5

Analytical techniques

Sample powders were fused in lithium-tetraborate and analysed for major and trace elements by means of X-ray fluorescence spectroscopy. FeO was measured titrimetically. Fe_2O_3 (actual) was calculated as Fe_2O_3 (e.g. XRF) minus (peO (titrimetically) * 1.112). In the case of microprobe analyses where usually all Fe is treated as FeO, the FeO (titrimetically determined on mineral separates) was subtracted from FeO (microprobe analyses) and the remaining FeO was treated as Fe_2O_3. LOI was determined gravimetrically at 1050°C. REE were determined with AES-ICP techniques using a Na_2O_2 decomposite following separation on cation exchange columns. The precision is better than 3% for major elements (except P_2O_5, MnO and Na_2O), generally better than 10% for REE, and better than 5-10% for other trace elements. Accuracy was controlled by the use of several international and in-house standards and the results are in good agreement with their recommended values. Major element composition of minerals were determined with an automated CAMECA microprobe at the University of Bonn, operating at 15 kV, 15 nA and using the ZAP correction procedure. Oxygen isotope analyses were performed at the University of Bonn on aliquots of powdered whole-rock samples, using purified fluorine as a reagent for oxygen extraction followed by conversion to CO_2 similar to the procedure described by Clayton and Mayeda (1963). $^{18}O/^{16}O$ measurements were made on a SIRA-9 triple-collector mass spectrometer by VG-Isogas.

Metamorphic conditions and estimation of P, T, X_{H2O} and f_{O2}

The rocks were finally metamorphosed under conditions beyond the K-feldspar-Al_2SiO_5 isograd. The assemblage cordierite-sillimanite-garnet-K-feldspar indicates a relatively low reaction pressure. The close relationship between the growth either of garnet or cordierite, the disappearance of some biotite and sillimanite, the development of *in-situ* leucosomes and the occurrence of partial melting on a regional scale either by the reaction:

bio + silli + qtz <-> cd + kf + gt + H_2O (1) or,
bio + cd + plg + Kf + qtz + H_2O <-> gt + melt (2)

support an anatectic origin for the *in-situ* leucosomes and suggest that garnet and sometimes cordierite were generated during incongruent melting of biotite and represent restitic phases within the leucosomes. Pressures and temperatures of high-grade metamorphism were estimated from the compositions of garnet, cordierite, biotite and plagioclase in migmatites and granites (Table 1) using calibration data of several authors (Table 2). In a recent review, Kleemann and Reinhard (1994) have shown that among the various calibrations for the garnet-biotite thermometer the calibration of Perchuk and Lavrent'eva (1983), which takes the non-ideality mixing behaviour of Al and Ti in biotite into account, gives reasonable temperature estimates and may therefore be used for calculating temperatures in high grade metamorphic rocks. In addition, the Al-in-hornblende geothermobarometer was used for estimating P/T conditions of emplacement of the hornblende-bearing granites. The estimation of X_H2O is based on the work of Osanai *et al.* (1991) and is presented in Fig. 1. Following Wones and Eugster (1965) oxygen fugacity was estimated from the Mg^{2+}, Fe^{2+}, Fe^{3+} composition of biotite in the *in-situ* leucosomes from the migmatites. The Fe/(Fe+Mg) ratio of 0.70 for the biotites corresponds to an oxygen fugacity of log $-f_O2 = -16$ at temperatures of 710°C, which was the maximum temperature obtained by geothermometry. The location of the biotite composition in the Fe^{3+}-Fe^{2+}-Mg^{2+} ternary diagram of Wones and Eugster (1965) corresponds to conditions between the QFM and NNO buffers.

Geochemistry of the host rocks

Major- and trace element composition and oxygen isotopic composition of representative samples are given in Table 3.

Metasediments

Pelites are Si-, Ca-, Na-poor and Al-, Fe-, Mg-, K- and Ti-rich and have a composition close to that of the average shales. This is further supported by their rather nonnal pelite-index (PI:(SiO_2/4)+2Al_2O_3+K_2O-(FeO+ Fe_2O_3+ MgO), Hoernes and Van Reenen, 1992) of 44

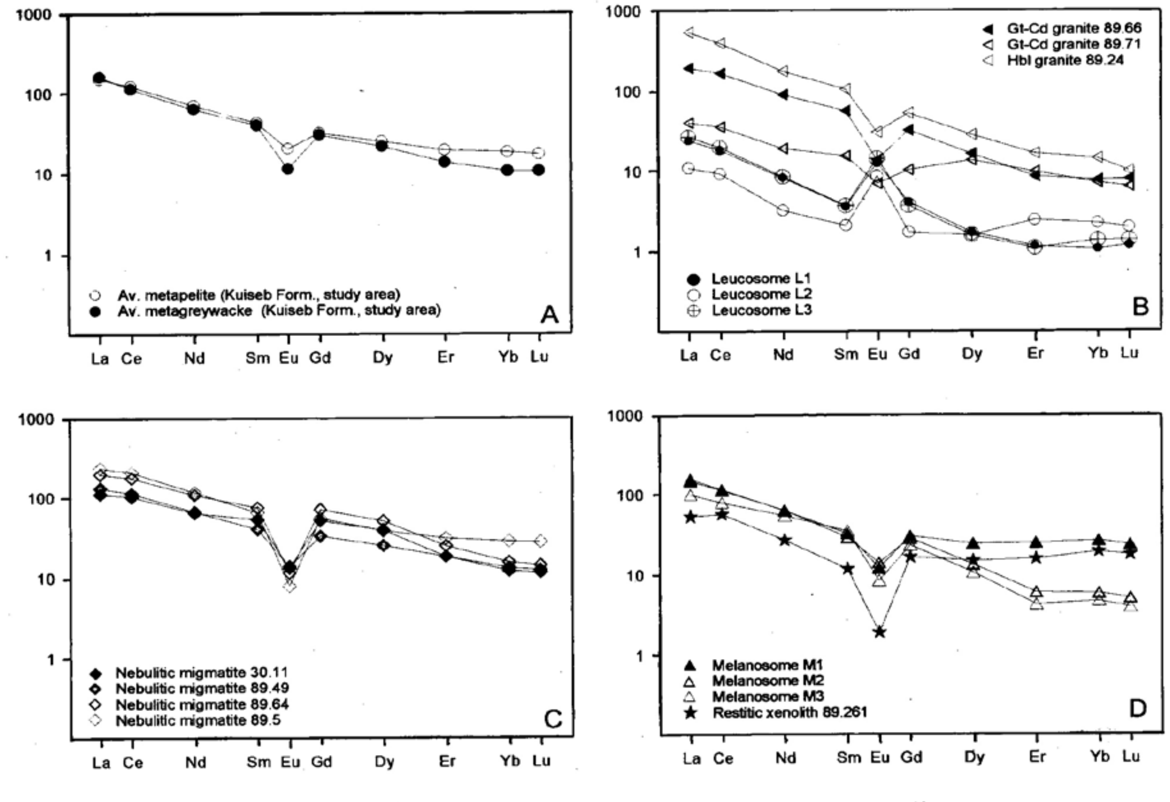

Figure 2: Chondrite-normalized REE composition of the investigated samples. A: Average pelite and metagreywacke from the Kuiseb Formation in the study area (Jung, 1994), B: garnet-cordierite granites, hornblende granite and *in-situ* leucosomes of the garnet-bearing stromatic migmatites, C: nebulitic garnet-free migmatites, D: Melanosomes of the garnet-bearing stromatic migmatites and one example of a restitic garnet- and cordierite bearing xenolith from the garnet-cordierite granites. Normalization values after Sun and McDounough (1989).

(Table 2) and their K/Rb ratio of 132, although the latter is somewhat lower than the average of pelitic rocks (K/Rb: 175, Taylor and McLennan, 1985). They have total REE contents of 174 ppm and display a fractionated REE pattern (La_N/Yb_N: 8.85) and a pronounced negative Eu anomaly (Eu/Eu*: 0.56, Fig. 2a). Their REE characteristics are close to the values given by Taylor and McLennan (1985) for various post-Archaean shales (REE: 173-204 ppm, La_N/Yb_N: 7.0-9.2, Eu/Eu*: 0.66-0.70).

Metagreywackes are enriched in Si, Ca and Na and depleted in Al, Ti, Fe, Mg and K relative to the pelites. The pelite-index of 40 is slightly lower than that for the pelites. The total REE content is somewhat lower (163 ppm), but the REE fractionation (La_N/Yb_N: 14.92) and the negative Eu-anomaly (Eu/Eu*: 0.34) are more pronounced than in the pelites. Total REE contents and LREE/HREE fractionation are close to the average of quartz-intermediate greywackes (REE: 130-176 ppm, La_N/Yb_N: 8.4-14.8) given by Taylor and McLennan (1985) but the negative Eu anomaly is more pronounced in the Damaran metagreywackes (Eu/Eu*: 0.38, quartz-intermediate greywackes: 0.69-0.75).

Pelites and metagreywackes have relatively low $\delta^{18}O$ values of 12.7 ± 0.9‰ and 11.8 ± 1.0‰ respectively which are significantly lower than the average of 14.0± 0.7‰ of Damaran pelites given by Hoernes and Hoffer (1985).

Granites

Granites derived from intra-crustal sources have a distinctive geochemistry (Miller, 1985). In the study area, the granites are characterized by high SiO_2, Al_2O_3 and Rb but moderate to high K_2O, Na_2O and Ba, moderate Sr, Pb and low FeO(tot) and MgO. Transition elements (Ni, Co, Cu, Cr, V, Sc) are low, Zr, Y and Nb show no systematic variation and Ga is high. Primary, unfractionated granites (sample 89.66) have rather normal total REE contents (212 ppm), a fractionated REE pattern (La_N/Yb_N: 25.33) and a pronounced negative Eu anomaly (Eu/Eu*: 0.33, Fig. 2b.). The molecular $Al_2O_3/CaO+Na_2O+K_2O$ ratio (A.S.I.: alumina saturation index Shand, 1949) is always greater than 1.10 and is therefore typical for peraluminous granitoids (Chappel *et al.*, 1987). Thus, the overall geochemistry of the granites displays all the features of S-type granites. Some of the intrusive granites have higher Na_2O and CaO and lower K_2O, lower Rb and Ba contents than the above described S-type granites. They have much lower total REE contents (51 ppm) and a less fractionated REE pattern which results in a lower La_N/Yb_N ratio (La_N/Yb_N: 5.68, sample 89/71 in Fig. 2b). The S-type granites have high oxygen isotopic compositions of 13.2‰ and 14.3‰. In contrast, the hornblende-bearing granite has lower SiO_2, higher FeO(tot), MgO and CaO but similar Al_2O_3, K_2O and Na_2O and consequently a lower alumina saturation index of 1.05. Rb contents are somewhat lower but Sr contents are high and Ba is very high relative to the garnet-cordierite granites. The Ga contents are lower than in S-type granites. The most distinctive feature is the relative enrichment of HFS elements, like Zr, Nb, Y, and the REE. Overall, they show a strongly fractionated REE pattern (La_N/Yb_N: 38.26) and a moderate negative Eu-anomaly (Eu/Eu*: 0.43, sample 89/24 in Fig 2b.). The oxygen isotopic composition of 11.87‰ is lower than in the S-type granites. In conclusion, this granite appears to have an A-type character.

Nebulitic garnet-free migmatites

The nebulitic garnet-free migmatites (samples 30.11, 89.49, 89.64, 89.5), which do not show the prominent leucosomes of the stromatic garnet-bearing migmatites, have SiO_2 contents identical to or somewhat lower than the pelites. In comparison with the pelites, they have higher TiO_2, lower Na_2O and variable Al_2O_3, FeO(tot), K_2O and Rb (255-544 ppm), Sr (5-94 pprn) and Ba (112-543 ppm) contents. The K/Rb ratio varies between 74 and 129. Total REE contents are similar to or higher than totals for the metasediments (155-281 ppm). The fractionation of LREE relative to HREE is similar (La_N/Yb_N: 8.18-12.46), but the negative Eu anomaly is more pronounced (Eu/Eu*: 0.14-0.25, Fig. 2c.) in the migmatites. The oxygen isotopic composition covers the range of the pelites and meta-greywackes.

Garnet-bearing migmatites

Melanosomes

The melanosomes (samples M1 - M3) of the garnet-bearing migmatites are depleted in SiO_2, CaO, Na_2O and Sr and enriched in TiO_2, Al_2O_3, MgO, K_2O, Rb, Ba, Y, Zr and transition elements relative to pelitic greywackes. Total REE contents are comparable to those in the metasediments and the nebulitic garnet-free migmatites but the negative Eu-anomaly is more pronounced than in the metasediments and is as low as that in the nebulitic migmatites (Eu/Eu*: 0.29-0.34, Fig 2d.). A restitic garnet-and cordierite-bearing xenolith (sample 89/261) from the garnet-cordierite granite, which is probably genetically linked to the garnet-bearing migmatites, is enriched in Al_2O_3 and FeO(tot), but strongly depleted in CaO, Na_2O, K_2O, Rb, Ba, Pb, Sr and total REE. Although garnet effects a relative enrichment of HREE, the fractionation between LREE and HREE is moderate but the strong negative Eu anomaly (Eu/Eu*: 0.16) is still present (Fig. 2d).

Leucosomes

The *in-situ* leucosomes (samples L1 - L3) of the garnet-bearing migmatites have a major- and trace element geochemistry which is very different from the

Table 3.: Major- and trace element composition of average metapelite, metagreywackes, nebulitic garnet-free migmatites (30/11, 89/49, 89/64, 89/5) melanosomes of garnet-bearing migmatites (M 1 - M 3), restitic xenolith (89/261), selected S-Type granites (89/66, 89/71) and a-type granites (89/24) as well as in-situ leucosomes (L 1 - L 3).

sample	Av. Meta-pelite	Av. Meta-greywacke.	neb. Mig. 30/11	neb. Mig. 89/49	neb. Mig. 89/64	neb. Mig. 89/5	Mig. Mel. 30.12 M1	Mig. Mel. 30.12 M2	Mig. Mel. 30.12 M3	Restite xenol. 89/261	s-type granite 89/66	s-type granite 89/71	a-type granite 89/24	Mig. Leuco. 30.12 L1	Mig. Leuco. 30.12 L2	Mig. Leuco. 30.12 L3
SiO_2	60,11	70,50	54,48	51,59	60,90	55,52	59,68	61,39	63,74	59,89	71,49	71,40	70,55	74,57	73,77	74,19
TiO_2	0,98	0,77	1,54	1,89	1,08	1,25	1,26	1,11	1,00	0,07	0,30	0,26	0,47	0,19	0,15	0,20
Al_2O_3	18,09	13,20	18,78	18,43	17,39	20,76	18,97	19,30	17,74	22,56	14,59	16,24	14,29	15,45	15,69	16,06
Fe_2O_3	0,89	0,87	2,14	1,11	1,51	1,43	1,39	1,11	1,70	1,12	0,25	0,15	0,24	0,22	0,10	0,27
FeO	6,82	3,88	6,82	9,67	6,25	9,38	7,39	5,48	5,12	6,42	1,55	1,88	2,48	1,02	1,41	1,05
MnO	0,11	0,05	0,08	0,10	0,09	0,24	0,17	0,07	0,08	0,34	0,03	0,03	0,04	0,01	0,03	0,01
MgO	3,92	2,13	3,62	3,54	3,44	4,86	3,42	2,69	3,04	4,24	0,53	0,74	0,78	0,44	0,40	0,50
CaO	0,75	1,11	0,92	0,78	1,59	0,09	1,04	0,97	0,60	0,23	1,05	1,47	2,05	1,69	1,93	1,89
Na_2O	1,65	2,81	1,53	1,13	2,14	0,44	2,51	2,72	1,83	0,90	2,74	4,31	2,98	4,25	4,71	4,52
K_2O	4,12	2,49	7,57	8,39	2,86	3,13	3,76	4,98	4,65	0,60	5,27	2,20	4,58	2,38	1,82	1,97
P_2O_5	0,15	0,11	0,71	0,60	0,64	0,06	0,08	0,10	0,09	0,01	0,18	0,15	0,12	0,09	0,08	0,09
LOI	2,10	2,10	2,01	1,51	1,99	2,07	1,63	1,51	1,77	3,68	0,89	1,09	0,92	0,60	0,48	0,59
total	99,69	100,00	100,20	98,74	99,88	99,23	101,30	101,43	101,36	100,06	98,87	99,92	99,50	100,91	100,57	101,34
∂18O	12,66	11,75	11,48			13,02				13,19	14,31	13,15				
A.S.I.											1,20	1,34	1,05	1,22	1,19	1,23
K/Rb	132	101	129	128	93	74	110	145	140	20	199	192	197	299	244	264
P.I.	44	40	46	44	42	43	44	50	46	49						
Li	130	62	80	n.d.	n.d.	n.d.	100	70	140	n.d.	51	90	n.d	31	29	32
Rb	260	205	486	544	255	353	285	285	275	255	220	95	193	66	62	62
Zn	169	120	265	263	218	297	233	200	205	50	70	53	62	41	41	44
Co	20	20	36	31	20	20	20	17	16	3	3	3	6	3	3	3
Cu	11	25	39	11	100	14	37	19	15	3	8	5	25	17	20	38
Ni	53	32	55	51	56	52	35	31	30	5	5	6	12	9	8	11
Pb	34	23	58	49	27	16	22	42	20	71	33	27	26	25	22	27
Sr	94	65	71	94	48	5	49	70	53	45	70	80	297	90	104	105
V	160	84	148	36	116	186	151	132	105	3	25	25	33	28	25	26
Ba	583	148	543	524	112	120	175	470	425	145	224	41	1426	170	110	150
Y	44	32	53	44	63	66	34	12	8	15	13	100	37	2	2	2
Cr	109	68	106	120	92	144	110	96	89	7	11	9	15	18	14	15
Zr	217	217	238	265	280	326	260	235	205	75	174	88	341	75	60	82
Nb	21	24	58	61	31	50	34	12	10	15	19	15	27	5	2	3
Sc	18	11	16	36	13	29	26	16	15	6	3	5	4	2	2	2
Ga											25	25	20	20	23	20
Rb/Sr											3,14	1,19	0,65	0,73	0,60	0,59
Sr/Ba											0,31	1,95	0,21	0,53	0,95	0,70
Rb/Ba											0,98	2,32	0,14	0,39	0,56	0,41
La	36,36	38,75	26,40	31,50	46,90	55,90	37,20	35,30	23,80	12,60	45,90	9,50	128,00	5,70	2,60	6,30
Ce	76,42	70,70	62,90	69,60	109,00	128,00	70,70	69,30	48,60	34,80	102,00	21,60	241,00	11,12	5,70	12,00
Nd	33,42	30,10	30,10	31,20	50,90	54,80	29,40	29,60	25,40	12,70	41,60	8,90	81,70	3,85	1,50	3,95
Sm	6,61	6,20	8,22	6,22	11,50	9,97	4,98	4,47	5,40	1,81	8,53	2,35	15,90	0,55	0,32	0,56
Eu	1,20	0,68	0,78	0,82	0,68	0,47	0,70	0,82	0,49	0,11	0,79	0,40	1,74	0,72	0,50	0,82
Gd	6,66	6,30	10,70	6,90	14,70	11,40	6,20	5,80	4,80	3,40	6,50	2,10	10,70	0,83	0,35	0,75
Dy	6,44	5,60	10,10	6,50	13,10	9,90	6,20	3,40	2,70	3,80	4,10	3,40	7,10	0,43	0,40	0,40
Er	3,28	2,30	3,10	3,10	4,20	5,20	4,10	1,00	0,70	2,60	1,40	1,60	2,70	0,19	0,40	0,18
Yb	3,18	1,85	2,10	2,30	2,70	4,90	4,50	1,00	0,80	3,30	1,30	1,20	2,40	0,18	0,38	0,23
Lu	0,45	0,28	0,30	0,32	0,37	0,72	0,60	0,13	0,10	0,45	0,20	0,16	0,25	0,03	0,05	0,04
Lan/Ybn	8,85	14,92	9,02	9,82	12,46	8,18	5,93	25,32	21,34	2,74	25,33	5,68	38,26	22,71	4,91	19,65
Eu*	0,56	0,34	0,25	0,39	0,16	0,14	0,34	0,42	0,29	0,16	0,33	0,53	0,43	2,09	2,74	2,54
SEE tot	174	163	155	158	254	281	165	151	113	76	212	51	491	24	12	25

intruding granites. Compared to the primary garnet-cordierite granite, the *in-situ* leucosomes have higher SiO_2, CaO and Na_2O, lower TiO_2, FeO, K_2O, P_2O_5 and similar contents of Al_2O_3 and MgO. Whereas the majority of these garnet-cordierite granites have K_2O>Na_2O, the *in-situ* leucosomes have Na_2O>K_2O. In comparison with some of the garnet-cordierite granites which show also Na_2O>K_2O, the *in-situ* leucosomes have higher SiQz and CaO, lower TiO_2, Al_2O_3, FeO and MgO and similar contents of Na_2O and K_2O. These geochemical differences are more pronounced with respect to trace elements. In comparison with the garnet-cordierite granites with K_2O>Na_2O, the *in-situ* leucosomes show lower Li, Rb, Pb, Ba, Y, Zr, Nb and Sc contents, higher Cu, Ni and Cr contents and roughly similar contents of Sr and V. The most striking features are the low total REE content and the positive Eu anomaly of the *in-situ* leucosomes, which separates them from the garnet-cordierite granites (Fig. 2b.). Compared to the granites with Na_2O>K_2O, the leucosomes have lower Li, Rb, Y and Nb, higher Cu, Ni, Co and Ba and similar contents of Sr, V, Pb, Zr and Ga.

Mineral chemistry

Based on field relationships and petrographic observations different generations of garnet and probably cordierite can be distinguished. These different mineral phases together with compositions of associated plagioclase and biotite are given in Table 1.

Garnet, cordierite, biotite and plagioclase, as well as K-feldspar (not reported here) from the migmatites exhibit no zoning, suggesting high-temperature equilibration. All garnets fall in the almandine field with minor amounts pyrope in solution and lesser quantities of spessartine and grossular. In the present case study mesosomes contain no pre-melting garnet. The granite veins, leucosomes and melanosomes provide garnets with distinct petrogenetic histories which is reflected in their contrasting major-element geochemistry. Garnets from leucosomes and melanosomes of the garnet -bearing migmatites are unzoned. Garnets from the leucosomes contain more of the spessartine component and, to a lesser extend, from the pyrope component than garnets from the melanosomes (columns 1-4, Table 1). Those garnets may be products of the incongruent dehydration melting of biotite. Euhedral garnets from the granites exhibit a pronounced zoning from pyrope-rich, spessartine-poor cores to pyrope-poor, spessartine-rich rims (columns 5-6 and 9-16, Table 1). This zoning is interpreted as being due to magmatic crystallization (e.g. Allen and Clarke, 1981; Phillips *et al.*, 1981; DuBray, 1988). Anhedral garnets with variable amounts of inclusions and sometimes pronounced haloes of quartz and plagioclase, which suggest growth after the peak of metamorphism, are only slightly zoned (columns 7-8, Table 1). Like the euhedral garnets, those garnets cores have lower spessartine and higher pyrope and grossular contents than the rims. Due to the higher grossular content, which suggest slightly higher pressures, these garnets may be refractory crystals from deeper crustal levels (e.g. Pattison *et al.*, 1982).

Biotites are members of the phlogopite-annite solid solution series with only small differences in the Al-content. Biotites of leucosomes contain less TiO_2 than those of the melanosomes. Biotites from the garnet-cordierite granite have surprisingly high TiO_2-contents, comparable with those from the melanosomes of the migmatites (columns 17-24, Table 1).

Cordierites from the migmatites are FeO-rich and show slightly higher Na_2O contents than cordierites from metasediments. The latter have roughly equal amounts of FeO and MgO (columns 33-35, Table 1). FeO enrichment and higher Na_2O contents in cordierites suggests a high-temperature origin for these cordierites, probably linked with an anatectic overprint (Speer, 1981; Flood and Shaw, 1975). Cordierites from the garnet-cordierite granites are FeO-rich with high contents of Na_2O, indicating a magmatic origin (column 36, Table 1).

Plagioclase in the hornblende granite falls in the composition field of andesin whereas that in the garnet-cordierite granite is an oligoclase (columns 25-32, Table 1).

Amphibole from the hornblende granite is pargasitic to ferro-pargasitic hornblende according to the nomenclature of Leake (1978).

Discussion

Field evidence and P-T estimates indicate that conditions for partial melting of mainly pelitic greywackes and formation of leucogranitic melts were attained during Damaran regional metamorphism in the study area.

Beside the results from geothermobarometry, the occurrence of different types of garnet within the garnet-cordierite granites offers the opportunity for the evaluation of the decompression and cooling history of the migmatite complex. The location of the individual samples of the garnet-cordierite granites in Fig. 1, the high grade conditions obtained from the compositions of the cores of the garnets and the matrix biotites and plagioclases as well as the core-rim relationship of individual garnets (following Martignole and Nantel, 1982) suggests that early in the metamorphic history a nearly isothermal decompression path was attained (samples 89/19, 89/80). In this case, isothermal decompression under relatively high grade metamorphic conditions (770°C/7.0 kbar, X_{H2O}: 0.4 to 740°C/5.3 kbar, X_{H2O}: 0.5) is an effective way for generation of granitic melts in the deeper crust. Later in the metamorphic history the migmatite complex evolved through isobaric cooling (740-760°C/4.2-4.6 kbar, X_{H2O}: 0.8; samples 26/5, 89/53-54) and unloading cooling (700°C, 4.4-5.6 kbar, X_{H2O}: 0.9, samples 12/2, 89/76, 30/12). Temperatures of 740-760°C and pressures of 5.6-7.0 kbar are believed to be remnants of high grade conditions in the deeper crust whereas temperatures of 690-710°C at 4.5 kbar reflect maximum PT conditions of high grade regional metamorphism.

The occurrence of at least four different types of granitic rocks (garnet-cordierite granites with $K_2O>Na_2O$ and $Na_2O>K_2O$, hornblende granites, *in-situ* leucosomes) together with abundant migmatites and unaffected metasediments offers the possibility to discuss the composition of leucosomes and intrusive granites in terms of partial melting processes of common crustal rocks. Petrogenetic investigations of migmatites and granites require modelling of trace elements and REE variations. However, disequilibrium behaviour of accessory phases during melting has critical consequences for trace element distribution in granites. The distribution of Rb, Ba, Sr which are controlled by major mineral phases (feldspars, biotite) and P, REE and Zr which are controlled by accessory phases (apatite, monazite, zircon) are commonly used to make constraints on the evolution of granitic melts.

Anatexis in the lower crust with a melt fraction higher than the minimum melt fraction (30-50%) has occurred to produce ‘the intrusive granites. The critical melt fraction forms at the point at which partially molten rocks change from granular framework to dense suspension behaviour (Wickham, 1987). In this case, the evolution of granites is consistent with the melt-restite model from Chappell *et al.* (1987), explaining the large amount of restite minerals (garnet, cordierite, sillimanite) in most of the garnet-cordierite granites. This feature may also explain the high alumina-saturation index. Furthermore, the geochemistry of these granites can be expressed in terms of fractional melting of metagreywackes (granites with $Na_2O>K_2O$) and pelites (granites with $K_2O>Na_2O$). Geochemical modelling, using typical Damaran Kuiseb Formation pelites and metagreywackes as the source rocks and abundant cordierite- and garnet-bearing restites within the granites as the residual rocks, implies unusually high degrees of partial melting (60-80% melt fraction) (Jung, 1994). The oxygen isotopic composition shows that the garnet-cordierite granites are typical crustal melts. Alteration, assimilation and fractional crystallisation are commonly assumed to be responsible for the shift to high $\delta^{18}O$ values of S-type granites (e.g. Taylor and Sheppard, 1986). No macroscopic nor microscopic evidence of alteration were observed and the negative correlation between the alumina-saturation-index and $\delta^{18}O$ values (not shown in detail here) preclude or fractional crystallisation as the major process for generating high $\delta^{18}O$ values. We assume that the high $\delta^{18}O$ values are primary values and the results of partial melting of highly evolved metasediments. Taking a $\delta^{18}O$ value of 14.0‰ for the average pelite as the source rocks (Hoernes and Van Reenen, 1992), it could be expected that partial melting produces granitic melts enriched in $\delta^{18}O$. Nevertheless, the relatively low $\delta^{18}O$ values of the investigated metasediments and migmatites in the studied area preclude such rocks as the source for the intrusive granites.

Miller (1985) and Harris and Inger (1992) have shown that Rb/Ba, Rb/Sr and Sr/Ba ratios can be used to place constraints on the source rocks of granitic magmas. According to Miller (1985), granites resulting from partial melting of pelitic sources have lower Rb, and Ba contents and similar Sr contents than their protoliths and Rb/Ba ratios >0.25. To the authors knowledge there are no comprehensive trace element data for typical Kuiseb Formation pelites (for 60% SiO_2 and $K_2O>Na_2O$) but taking averages of 260 ppm Rb, 580 ppm Ba and 100 ppm Sr for the Kuiseb Formation pelites from the study area into account (n=7, Jung, 1994 and unpublished data) the primary garnet-cordierite granites (220-260 ppm Rb, 220-250 ppm Ba, 70-100 ppm Sr) fulfil these criteria.

According to Harris and Inger (1992), granitic melts generated by the incongruent melting of muscovite are characterized by low Rb/Sr (0.7-1.6) and high Sr/Ba (0.5-1.6) ratios because the restite is depleted in feldspar. Furthermore, these melts indicate the presence of a vapour phase. In contrast, vapour-absent melting will result in the incongruent melting of biotite and high Rb/Sr (2-6) and low Sr/Ba (0.2-0.7) ratios in the melts. The intrusive granites, which have not experienced extensive crystal fractionation (e.g. sample 89.66) have a Rb/Ba ratio around 1.0, Rb/Sr of 2.60- 3.14 and Sr/Ba of 0.30-0.40 and are therefore products of dehydration melting processes of biotite-bearing pelites in the deeper crust.

It is generally assumed that incompatible elements preferentially partition into the melt during fusion. However, certain incompatible elements such as Zr, P and LREE, because they are essential structural components of accessory phases such as zircon, apatite and monazite, will be strongly partitioned into these phases in preference to the melt. The concentration of these elements is considered to be a good indication of the extent to which those accessory phases are consumed during melting or entrained in anatectic melts. Using the empirical equations for Zr, P_2O_5 and LREE saturation of Watson (1988) it is possible to obtain the saturation concentration for Zr, P_2O_5 and LREE for a typical peraluminous melt containing 73 wt % SiO_2 at a certain temperature. Typically unfractionated garnet-cordierite granites of the study area have 170 ppm Zr, 200 ppm LREE and 0.20 wt % P_2O_5. The application of the empirical equations mentioned above indicate equilibrium temperatures of around 800°C for Zr and 810°C for LREE. The application of the model from Harrison and Watson (1984) and the equation from Watson (1988) yield significantly lower P_2O_5 contents for 800°C or extremely high temperatures for equilibration (1000°C). Bea *et al.* (1992) pointed out the need for correction of the Harrison and Watson model, because of the increased solubility of P in Ca-poor, peraluminous melts. Application of the Bea *et al.* (1992) correction yields an equilibration temperature of 850°C for 0.19 wt %

P_2O_5, which seems to be more realistic. These temperature estimates are believed to represent temperatures of formation of the S-type granites and indicate that the primary garnet -cordierite granites are restite-poor melts with respect to zircon, apatite and monazite. Using the above mentioned empirical equations, saturation temperatures for the hornblende granites of 880°C for LREE, 900°C for P_2O_5 and 860°C for Zr were obtained and are in good agreement with previous estimates of initial temperatures for A-type granites (Clemens *et al.*, 1986). It is necessary to state that these temperature estimates more likely reflect initial temperatures in the lower crust during generation of both types of granites than metamorphic temperatures during high grade evolution of the complex.

Furthermore, some of the intrusive granites with $K_2O>Na_2O$ have experienced extensive crystal fractionation which can be modelled by fractionation of amphibole, biotite, plagioclase, monazite, allanite and sphene. The process of fractional crystallisation can be traced using the elements Zr, Rb, Sr, Ba and REE. The final products are differentiated rocks with the typical wing-shaped REE pattern which result from fractionation of LREE-enriched accessory phases, crystallisation and accumulation of alkali-feldspar and entrainment of phases like garnet with HREE>LREE (Miller and Mittlefehld, 1982; Shearer *et al.*, 1982).

During high-grade metamorphism anatexis of pelitic metagreywackes and extraction of low melt fractions has occurred. Most of the leucosomes of the garnet-bearing migmatites may have developed by such a process. The geochemistry of the migmatites, like variable K_2O, Na_2O, Rb, Sr and Ba values is consistent with limited extraction of a granitic melt. In this case, petrogenetic modelling suggests only a small degree of partial melting (15-25% melt fraction) of pelitic greywacke source rocks. The P, T, X_{H2O} and f_{O2} conditions (700°C, 4-5 kbar, X_{H2O}=0.9, log f_{O2}= -16 (between the QFM and NNO buffers, and therefore slightly reducing conditions)) support such an origin. Rb/Ba is 0.39-0.56, Rb/Sr is 0.59-0.73 and Sr/Ba is 0.50-0.95. These trace element ratios are characteristic of granitic melts generated by partial melting of metasedimentary rocks in the presence of a vapour phase. The maximum Zr content is 80 ppm, LREE is 22.8 ppm and P_2O_5 is 0.09 wt%. The calculation of equilibrium temperatures yielded 740°C for Zr, 650°C for LREE and 780°C for P_2O_5 and indicate that these leucosomes are probably melts which where generated under disequilibrium conditions. They contain a limited amount of restitic minerals. The possibility that these leucosomes are the differentiation products of the intrusive granites can be ruled out because of the pronounced fractionation of LREE over HREE (La_N/Yb_N: 20), the much lower positive Eu anomaly and the higher Cu, Co, Cr and Ni contents which are typical of unfractionated granitic melts generated from metasedimentary rocks.

Higher Sr and Ba contents and therefore different Rb/Ba, Rb/Sr and Sr/Ba ratios as well as higher contents of HFSE and REE in the hornblende granite point out to a non-metasedimentary source and it is suggested that the hornblende granite is the product of limited partial melting of a non-depleted lower crust, probably of tonalitic composition. Such melts can be generated late in the tectono-metamorphic evolution of an orogenic belt during advanced uplift and exhumation.

The genetic link between SiO_2-rich granitic leucosomes with positive Eu anomalies and low contents of trace elements (normally hosted in accessory phases) and normal S-type granites with elevated trace element contents and negative Eu anomalies lies in the different melting behaviour in the deeper crust and the different entrainment and solubility of accessory restitic phases. Low trace element contents and positive Eu anomalies may be indicative of disequilibrium melting of feldspar-rich material under nearly water-saturated conditions where melts are extracted from the restite before reaching chemical equilibrium. Additionally, the relatively dry peraluminous nature inhibits solution of accessory phases like zircon and monazite. As melting proceeds, larger masses of magma are mobilized and the entrainment (and probably the solution) of restitic phases is facilitated, resulting in trace element enriched S-type granites which can be found in all Phanerozoic mobile belts worldwide. Thus, a careful geochemical investigation, coupled with major and trace element modelling is necessary to understand the evolution of granitic rocks from low-melt fractions to high-melt fractions.

Acknowledgements

This work was funded by grants from the Deutsche Forschungsgemeinschaft to E. Hoffer (Ho 1078/1-2) and forms part of the Ph.D thesis of S.l. The authors are very grateful to Prof. Dr. Raith and Dr. B. Spiering/University of Bonn for making microprobe facilities available and for good advice and encouragement during several stays at Bonn. Constructive comments on an earlier version of the manuscript by D.L. Reid and R. McG. Miller are greatly appreciated and helped to improve the paper.

References

Allen, B.D. and Clarke, D.B. 1981. Occurrence and origin of garnets in the South Mountain batholith, Nova Scotia. *Can. Mineral.*, **19**, 19-24.

Bea, F. Fershtater, G. and Corretge, L.G. 1992. The geochemistry of phosphorus in granite rocks and the effect of aluminium. *Lithos*, **29**, 43-56.

Blundy, J.D. and Holland, T.J.B. 1990. Calcic amphibole equilibria and a new amphibole-plagioclase geotherrnometer. *Contrib. Mineral. Petrol.*, **104**, 208-224.

Brown, M. 1993. The generation, segregation, ascent and emplacement of granite magma: the migmatite-to-crustally derived granite connection in thickend orogens. *Earth Sci. Rev.*, **36**, 83-130.

Chappell, B.W., White, A.J.R. and Wyborn, D. 1987. The importance of residual source material (restite) in granite petrogenesis. *J. Petrol.*, **28**, 1111-1138.

Clayton R.N. and Mayeda, T.D. 1963. The use of bromine pentaflouride in the extraction of oxygen from oxides and silicates for isotope analysis. *Geochim. cosmochim. Acta*, **27**, 43 -52.

Clemens, J.D. and Vielzeuf, D. 1987. Constrains on melting and magma production in the crust. *Earth Planet Sci. Lett.*, **86**, 287-306.

Clemens, J.D., Holloway, J.R. and White, A.J.R 1986. Origin of an A-type granite: Experimental constrains. *Am. Mineral.*, **71**, 317-324.

Conrad, W.K., Nicholls, L.A. and Wall, V.J. 1988. Water-saturated and-undersaturated melting of metaluminous and peraluminous crustal compositions at 10 kb: evidence for the origin of silicic magmas in the Taupo Volcanic Zone, New Zealand, and other occurrences. *J. Petrol.*, **29**, 765-803.

DuBray, E.A. 1988. Garnet compositions and their use as indicators of peraluminous granitoid petrogenesis, southeastern Arabian Shield. *Contrib. Mineral. Petrol.*, **100**, 203-212.

Flood, R.H. and Shaw, S.E. 1975. A cordierite-bearing granite suite from the New England batholith, N.S.W., Australia. *Contrib. Mineral. Petrol.*, **52**, 157-164.

Ghent, E.D. 1976. Plagiociase-garnet-Al_2SiO_5-quartz: a potential geobarometer-geotherrnometer. *Am. Mineral.*, **61**, 710-714.

Harris, N.B.W. and Inger, S. 1992. Trace element modelling of pelite derived granites. *Contrib. Mineral. Petrol.*, **110**, 46-56.

Harrison, M.T. and Watson, E.B. 1984. The behaviour of apatite during crustal anatexis: Equilibrium and kinetic considerations. *Geochim. cosmochim. Acta*, **48**, 1467-1477.

Hoernes, S. and Hoffer, E. 1985. Stable isotope evidence for fluid-present and fluid-absent metamorphism in petites from the Central Damara Orogen, Namibia. *Contrib. Mineral. Petrol.*, **90**, 322-330.

Hoernes, S. and van Reenen, D.D. 1992. The oxygen-isotopic composition of granulites and retrogressed granulites from the Limpopo Belt as a monitor of fluid-rock interaction. *Precambr. Res.*, **55**, 353-364.

Holdaway, M.J. and Lee, S.M. 1977. Fe-Mg cordierite stability in high grade pelitic rocks based on experimental, theoretical and natural observations. *Contrib. Mineral. Petrol.*, **63**, 175-198.

Hollister, L.S., Grissom, G.C., Peters, E.K., Stowell, H.H. and Sisson, V.B. 1987. Confirmation of the empirical correlation of Al in hornblende with pressure of solidification of calc-alkaline plutons. *Am. Mineral.*, **72**, 231-239.

Holtz, F. and Barbey, P. 1991. Genesis of peraluminous granites. II. Mineralogy and chemistry of the Tourem Complex (North Portugal). Sequential melting vs. restite unmixing. *J. Petrol.*, **32**, 959-978.

Holtz, F. and Johannes, W. 1991. Genesis of peraluminous granites. 1. Experimental investigation of melt composition at 3 and 5 kb and various H_2O activities. *J. Petrol.*, **32**, 935-958.

Jung, S. 1994. *Geochemische und petrologische Untersuchungen an Metagraniten, Migmatiten und Metasedimenten des zentralen Damara Orogens, Namibia*. Ph.D. thesis (unpubl.), Univ. Marburg, Germany, 187 pp.

Johnson, M.C. and Rutherford, M. J. 1989. Experimental calibration of the aluminium-in-hornblende geobarometer with application to Long Valley caldera (California) volcanic rocks. *Geology*, **17**, 837-841.

Kleemann, U. and Reinhardt, J. 1994. Garnet-biotite thermometry revisited: the effect of Al^{IV} and Ti in biotite. *Eur. J. Mineral.*, **6**, 925-941.

Leake, B.E. 1978. Nomenclature of amphiboles. *Can. Mineral.*, **16**, 501-520.

LeBreton, N. and Thompson, A.B. 1988. Fluid-absent (dehydration melting) of biotite in pelites in the early stages of crustal anatexis. *Contrib. Mineral. Petrol.*, **99**, 226-237.

Martignole, J. and Nantel, S. 1982. Geothermobarometry of cordierite-bearing pelites near the Morin anorthosite complex, Grenville Province, Quebec. *Can. Mineral.*, **20**, 307-318.

Miller, C.F. 1985. Are strongly peraluminous magmas derived from pelitic sedimentary sources? *J. Geol.*, **93**, 673-689.

Miller, C.F. and Mittlefehldt, D.W. 1982. Depletion of light rare-earth elements in felsic magmas. *Geology*, **10**, 129-133.

Osanai, Y., Komatsu, M. and Owada, M. 1991. Metamorphism and granite genesis in the Hidaka Metamorphic Belt, Hokkaido, Japan. *J. metamorph. Geol.*, **9**, 111-124.

Otten, M.T. 1984. The origin of brown hornblende in the Artfjallet gabbro and dolerites. *Contrib. Mineral. and Petrol.*, **86**, 189-199.

Pattison, D.R.M., Carmichael, D.M. and St-Onge, M.R. 1982. Geothermometry and Geobarometry applied to early Proterozoic “S-type” granitoid plutons, Wopmay Orogen, Northwest Territories, Canada. *Contrib. Mineral. Petr.*, **79**, 394-404.

Perchuk, L.L. and Lavrent’eva, I.V. 1983. Experimental investigation of exchange equilibria in the system cordierite-garnet-biotite. *In*: Saxena, S.K. (Ed.), *Kinetics and Equilibrium in Mineral Reactions*, Springer, Berlin, 199-239.

Perchuk, L.L., Podlesskii, K.K. and Aranovich, L.Y. 1981. Calculation of thermodynamic properties of endmember minerals from natural paragenesis. *In*: Newton. R.C., Navrotsky. A., and Wood. B. J. (Eds), *Advances in Physical Geochemistry*. Thermodynamics of Minerals and Melts. Springer, Berlin, 131-147.

Perchuk, L.L., Aranovich, L.Y., Podlesskii, K.K., Lavrenteva, 1. V., Gerasimov, V. Y. and Fedkin. V.V. 1985. Precambrian granulites of the Aidan shield, Eastern Siberia, USSR. *J. metamorph. Geol.*, **3**, 265-310.

Phillips, G.N., Wall, V.J. and Clemens, J.D. 1981. Petrology of the Strathbogie batholith: a cordierite bearing granite. *Can. Mineral.*, **19**, 47-63.

Powell, R. and Holland, T.J.B. 1988. An internally consistent dataset with uncertainities and correlations: 3. Application to geobarometry, worked examples and a computer program. *J. metamorph. Geol.*, **6**, 173-204.

Price, R.C. 1983. Geochemistry of a peraluminous granitoid suite from north-eastern Victoria, south-eastern Australia. *Geochim. cosmochim. Acta*, **47**, 31-42.

Shand, S.J. 1949. *Eruptive rocks, their genesis, composition, classification, and their relation to ore deposits*. T. Murby, London, 3rd edition, 488 pp.

Shearer, C.K., Papike, J.J., Redden, J.A., Simon, S.B., Walker, R.J. and Laul, J.C. 1987. Origin of pegmatitic granite segregations, Willow Creek, Black Hills, South Dakota. *Can. Mineral.*, **25**, 159-171.

Speer, J.A. 1981. Petrology of cordierite-and almandine-bearing granitoid plutons of the southern Appalachian Piedmont. *U.S.A. Can. Mineral.*, **19**, 35-46.

Sun, S.S. and McDonough, W.F. 1989. Chemical and Isotopic systematics of ocean basalts: implications for mantle composition and processes. *In*: Saunders, A.V. and Norry, N.J. (Eds), *Magmatism in the ocean basins*. Geol. Soc. London Spec. Publ., **42**, 313-345.

Taylor, S.R. and McLennan, S.M. 1985. The continental crust: its composition and evolution. *Blackwell*, London, 3112pp.

Taylor, Jr. H.P. and Sheppard, S.M.F. 1986. Igneous rocks: 1. Processes of isotopic fractionation and isotope systematics. *In*: *Stable isotopes in high temperature geological processes*. Rev. Mineral., **16**, 227-271.

Thompson, A.B. 1976. Mineral reactions in pelitic rocks: II. Calculation of some P-T-X (Fe-Mg) phase relations. *Am. J. Sci.*, **276**, 425-454.

Thompson, A.B. 1982. Dehydration melting of pelitic rocks and the generation of H_2O-undersaturated granitic liquids. *Am. J. Sci.*, **282**, 1567-1595.

Vielzeuf, D. and Holloway, J.R. 1988. Experimental determination of the fluid-absent melting relations in the pelitic system. Consequences for crustal differentiation. *Contrib. Mineral. Petrol.*, **98**, 257-276.

Vyhnal, C.R., McSween, Jr., H.Y. and Speer, A. 1991. Hornblende chemistry in southern Appalachian granitoids: Implication for aluminium hornblende thermobarometry and magmatic epidote stability. *Am. Minerals*., **76**, 176-188.

Watson, E.B. 1988. The role of accessory minerals in granitoid geochemistry (abstract). The origin of granites. R Soc. London, Hutton Meeting, Edinburgh, 19-20.

Wickham, S.M. 1987. The segregation and emplacement of granitic magmas. *J. Geol. Soc., London*, **144**, 281-297.

Wones, D. Rand Eugster, H. P. 1965. Stability of biotite: experiment, theory, and application. *Am. Mineral.*, **50**, 1228-1272.